

# Modification on Static Response Under Wind Load: Effects of Rectangular Tall Building Vertical Chamfered Edge

Adal Mengesha Yimer

Civil Engineering Department, Gafat Institute of Technology, Debre Tabor University, Debre Tabor, Ethiopia

**Email address:**

adalmengesha123@gmail.com

**To cite this article:**

Adal Mengesha Yimer. Modification on Static Response Under Wind Load: Effects of Rectangular Tall Building Vertical Chamfered Edge. *Journal of Civil, Construction and Environmental Engineering*. Vol. 8, No. 3, 2023, pp. 49-59. doi: 10.11648/j.jccee.20230803.12

**Received:** April 24, 2023; **Accepted:** June 21, 2023; **Published:** July 6, 2023

---

**Abstract:** Now adays, due to architectural and structural requirements, complicated tall and slender buildings with various corner configurations and cross-sectional shapes are emerged, which are difficult to design using the existing wind load standards as well as using available software packages. For such conditions, an experimental study is the best solution to develop new standards and solve such design limitations. In this study a total of five rigid plywood models of equal height are prepared at a scale of 1:100, the principal model is a rectangular building with the geometry of B\*D\*H, 200mm\*300mm\*500mm and other models are vertically chamfered edges as B/8, B/4, 3B/8, and B/2. In properly designed open rectangular boundary layer wind tunnel with 2m\*2m\*15m simulation section at IIT Roorkee, India. The model is placed on the top floor and the mean wind velocity profile of approaching flow 9.61m/sec corresponding to terrain Category-II is allowed to pass through the circuit and various digital signal readings are taken at various wind incidences then converted to forces, moment, coefficients and results are compared with existing codes. As vertical chamfering size increases, twisting and torsional moment increases, drag force coefficient and lift-force coefficient increase due to the slenderness of the chamfered building compared with the principal building.

**Keywords:** Chamfered Edge, Drag Coefficient, Lift Coefficient, Wind Load, Static Response

---

## 1. Introduction

Tall buildings have been traditionally designed to be symmetric rectangular, square, triangular as well as circular in plan, to avoid excessive seismic and wind-induced torsional vibrations due to eccentricity, in highly seismic prone and wind-induced regions.

Due to the rapid development of construction technology, very slender and tall buildings with unconventional and irregular geometric shapes in the plan as well as in elevation are constructed rapidly from time to time. Such unconventionality in shape and configuration may be due to architectural and structural requirements as well as engineers' need to show their professional excellence. The design of such unconventionally configured tall buildings using the usual building code of standards becomes challenging. Most countries like India, America, Asia, and Europe have wind load design codes for common geometric building shapes. For example, the Indian standard on wind loads IS: 875, Part-3-2015 gives external pressure coefficient values on square,

rectangular, circular, and some smooth-edged plan shape clad buildings at limited wind incidence angle. Since there is no Codal information available for the design of the unconventional tall building with various corner configurations and cross-sectional shapes, numerous experimental wind tunnel studies have been done to obtain the design force and pressure coefficients. This study is conducted to know the effect of vertical chamfering on rectangular tall buildings on the static response of wind load at various wind incidence angle using a wind tunnel experimental study. The result from this study will contribute as a design reference for such a building under wind load.

## 2. Objective of the Study

The main objective of this study is to investigate the effect of wind loads on vertical edge modification of rectangular tall buildings which is not addressed by most wind design codes.

### 3. Limitation of the Study

This study is primarily conducted on an open layer wind tunnel experimental set up based on IS: 875, Part-3-2015 only and also the effect of vertical edge chamfering does not taking into account on the architectural function of the building.

### 4. Literature Review

K.C.S Kwok 1998 studied the effect of wind on rectangular tall building using Wind tunnels. According to his study horizontal slots, slotted corners and chamfered corners caused significant reductions in both the along-wind and cross-wind responses and also he was examined the wake spectra, probability distributions of the responses, and the along-wind and cross-wind force spectra [1].

Amin, JA and Ahuja, Ashok Kumar conducted systematic review research on aerodynamic modifications to the shape of the buildings. This review paper presents an overview and a summary of past/recent work on various aerodynamic modifications to the shape of the buildings like corner cuts, chamfering of corners, rounding of corners, horizontal and vertical slots, dropping of corners, tapering, etc. to reduce the wind excitation of tall flexible buildings and its application in some of the tall buildings across the world [2].

Bhatnagar, N. K. 2011 investigated the effect of wind direction and calculate the total wind load on a square plan building with rectangular, cut, and chamfered (20mm\*20mm) corners with the height of 450mm and a cross-section of 100mm\*100mm having an aspect ratio, h/w of 4.5. The author measured base shear and base moment from 0° to 90° at three wind speeds namely 6.67, 8.27, and 10.12 m/s and compares base shear in X-direction (Fx) at 45° and found that maximum Fx occurs in the rectangular corner at 500rpm which was 300gm and minimum Fx at chamfered corner occurs at 300rpm which is 90gm [3].

J. A. Amin • A. K. Ahuja 2014, studied wind tunnel tests on rectangular building models having the same plan area and height but different side ratios of 1, 1.56, 2.25, 3.06 and 4 to know the characteristics of wind forces on rectangular tall building. the authors noted that the side ratio of buildings significantly affects the wind pressures on leeward & sidewalls, whereas wind pressure on windward wall is almost independent of side ratio. [4].

Mooneghi, Maryam Asghari and Kargarmoakhar, Ramtin, 2016, conducted a systematic literature review on aerodynamic mitigation and shape optimization of buildings for wind loads of related literature studied using wind tunnel experimental method and computational fluid dynamics approach. According to the author's review, the aerodynamic Modifications of a building's cross-sectional shape (e.g. corner cut, corner recession, slotted corner, etc.), variation of the cross-section shape and/or its size along with the height of the building, twisting the building, porosity, and openings, etc. can significantly reduce building response in along wind (drag force) as well as across-wind (crosswind force due to

vortex shedding) directions by altering the wind flow characteristics around the building [5].

Ashutosh, Sharma and Hemant, Mittal and Ajay, Gairola, 2018, conducted a systematic review on mitigation of wind load on tall buildings through aerodynamic minor modifications (corner cut, rounding, chamfer, etc.) and major modifications (taper, set-back, twist, etc.) by reviewing the recent/past aerodynamic modification techniques applied to high-rise buildings. From their review, the author summarizes Bluff shaped structures are more vulnerable to wind-induced excitations and can be controlled either by structural or aerodynamic modifications, Structural modifications consider the parametric adjustment of structural properties such as mass, stiffness, and damping, Minor modifications promote the shear layer reattachment and narrow down the wake width on the leeward side of the building and can result into a reduction of 30%-60% in wind-induced loads, on the other hand, major modifications can change the vortex shedding phenomenon throughout height [6].

Li, Yi and Li, Chao and Li, Qiu-Sheng and Song, Qian and Huang, Xuan and Li, Yong-Gui, 2020, examined aerodynamic performance of CAARC standard tall building with various corner chamfers. The authors considered Five rigid tall building models as benchmark models and four corners chamfered models with different modification rates from 5% to 20% and tested for pressure measurements in a boundary layer wind tunnel to know wind pressure coefficients, wind force coefficients, base moment coefficients, and their power spectral densities. The results show that the aerodynamic performance of the tall building models can be effectively improved as the corner chamfer rate increases. The authors also conclude that the Corner chamfers can effectively reduce both the mean and RMS drag coefficients and the power spectral densities of the along-wind forces are not sensitive to variation of corner chamfer rate [7].

Thordal, Marie Skytte and Bennetsen, Jens Chr and Capra, Stefano and Kragh, Andreas K and Koss, H Holger H, 2020 conducted a Blind test for chamfered and rounded corner high-rise buildings for wind load using a standard CFD setup. The authors conducted CFD simulations based on CAARC standards to study the mean surface pressure on the targeted model to check the consistency of the result as it was conducted by the wind tunnel experimental method. The result shows that the mean surface pressures on both high-rise buildings had high consistency with experimental results. Furthermore, the minimum and maximum peak surface pressure coefficients showed prominent good agreements. The chamfered high-rise building had average deviations of 14.92, 14.08, and 22.07% for the Mx, My, and Mz base peak moments respectively [8].

Mohammad Jafaria, and Alice Alipoura, 2020, perform a systematic research review Methodologies to Mitigate Wind-induced Vibration of Tall Buildings such as passive, active and semi-active on researches conducted by wind tunnel experiment and Computational Fluid Dynamics (CFD) [9].

Jamaluddeen and Rajiv Banerjee, 2021 surveys various research papers conducted on wind load effect on high rise building with various forms and configuration and they conclude that many research are not considering the dynamic effects of wind and the results of many papers are not translated to standards like design codes and manuals [10].

Astha Verma, Rahul Kumar Meena, Hrishikesh Dubey, Ritu Raj, and S. Anbukumar, 2022 investigated the effect of wind on building with equal area and equal height with different regular and irregular cross sectional shape. The numerical study is performed using ANSYS CFX and wind incidence angle of  $0^\circ$  to  $180^\circ$  at the interval of  $15^\circ$ . According to their study the regular shape with corner cut and 'Y' shape model with fillet corner shows better resistance to wind force than other models [11].

(Meena, Rahul Kumar and Raj, Ritu and Anbukumar, S, 2022) examined wind exited action around tall buildings having different corner configurations of a rectangular corner, corner cut, chamfered corner, and fillet shape corner using the wind tunnel experimental method. The author indicates that corner modification has a great advantage for wind load reduction and especially round corner edge has high reduction resistance in reducing along with wind forces [12].

(Al-masoodi, Aiman HH and Alkhatib, FH and Shafiq, N and Wahab, MMA, 2022) conducted a systematic literature review on the Aerodynamic performance of tall buildings through the utilization of aerodynamic modification techniques for tall buildings. The author concludes that recession and set-back type modifications are the most effective in wind load resistance and design modifications must be evaluated earlier in the design stage to mitigate the wind load effect and occupant's comfort [13].

Indian Standard, IS 875 (Part-3): 2015, provides positive and negative wind pressure coefficients for walls of rectangular clad building at critical wind directions as given in Clause 7.3.3.1 and overall force coefficients for clad buildings with uniform section of smooth, sharp, pointed edges at one principal wind direction only as given in Clause 7.4.2.2. But, this code does not provide wind load design information for building with various corner configuration at different wind incidences [14].

AS/NZS: 1170.2 (2002) is wind design code specifies pressure coefficients on windward and leeward walls of rectangular enclosed buildings for  $0^\circ$  and  $90^\circ$  wind directions only as given in Clause 5.4.1 and drag force coefficients for Sharp edged square, rectangular, triangular and multi-sided polygon prism shaped and round edged cylindrical buildings as given in Clause E 3.1 [15].

## 5. Research Methodology

### 5.1. Wind Tunnel Set up

The tests are conducted in an open circuit rectangular boundary layer wind tunnel of cross-section  $2\text{m} \times 2\text{m} \times 15\text{m}$  at IIT Roorkee. Flow roughening devices such as vortex

generators, barrier walls, and cubical blocks are used on the upstream end of the test section to achieve the mean wind velocity profile of approaching flow corresponding to terrain Category-II of IS: 875, Part-3-2015.

### 5.2. Equipments and Tools

For a complete experimental study, various equipment and tools were been used, such as Load-Cell, a five-component load-cell used to measure static responses of building namely, base force ( $F_x$ ,  $F_y$ ), base moment ( $M_y$ ,  $M_x$ ), and twisting moment ( $M_z$ ) under wind loads. Testo-480, a tool used to measure the variation of velocity and pressure inside the test section, Data Acquisition System, an electronic device that receives the electrical signal in the form of physical quantities like velocity, surface pressure, force, and displacement and converts the electrical signal into digital numeric values, Data-Taker (DT80), an instrument connected with five component load cell cables and with software loaded in the computer is used as Data Acquisition System for load-cell, Turn Table, a circular rotating surface installed below the test floor to place the model for testing and Scan valve an instrument with two storage banks each can read 64 pressures at a time, is used for surface pressure measurement.



Figure 1. Equipments and tools.

### 5.3. Flow Conditions

The test is conducted at the mean free stream wind velocity profile of approaching flow of  $9.61\text{m/sec}$ . The maximum mean turbulence intensity inside the test section is  $8.94\%$  which occurs at  $20\text{mm}$  above the test floor. The maximum blockage ratio of  $3.75\%$  is used for the test set up and the model considered.

### 5.4. Load Cell Calibration and Model Set up

The prototype principal tall building is assumed to have

B\*D\*H, 200mm\*300mm\*500mm dimension. The chamfered model is prepared by chamfering vertically the longer side of the rectangular building. The models are made of rigid plywood at a scale of 1:100. Each model is placed one by one on a calibrated load cell and tested under a free stream mean wind velocity of 9.1m/sec rotated at various wind incidences.

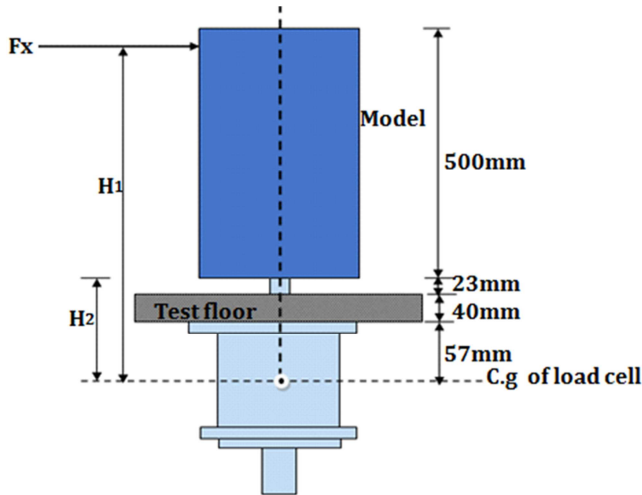


Figure 2. Set up and calibration of load cell.

### 5.5. Experimental Procedure

The wind tunnel set ups, flow condition, a plywood model, and force recording devices are properly adjusted before experimental readings. Then aerodynamic forces on all rigid models are measured using a five-component force balance which is fixed under the wind tunnel floor. The required flow

conditions of free stream mean wind velocities of 9.61m/sec inside the test section are established by placing flow roughening devices in upstream of the test section. Experimental observations are recorded for 60 seconds at an interval of 1 second from 0° to 180° rigid model position rotated at an interval of 15° and then static response data is recorded and interpreted.

### 5.6. Measurement Techniques

The force and moment readings in the display unit are taken in the form of a digital signal of mili-volt and then converted into gm and gm-mm by dividing those readings with calibration constants. To calculate the calibration constant for  $F_x$  and  $M_y$ , the load cell is loaded with a hanger of various weights applied in the direction of X in the absence of wind load. Calibration coefficients obtained from the calibration of load cell are -0.00234 for base shears, -0.0000101 for base moments, and -0.000038 for twisting moments.

The actual value of base force in the X and Y direction and twisting moment in the Z direction is calculated by dividing the reading from the load cell by the respective calibration coefficient, whereas the actual value of base moment in the X and Y direction is multiplied by the lever arm from the base to respective wind load location. Since the load cell gives a moment at the center of gravity of the load cell, the moment corrected by the calibration coefficient is multiplied by the lever arm from the base of the model to the location of load to obtain the base moment.

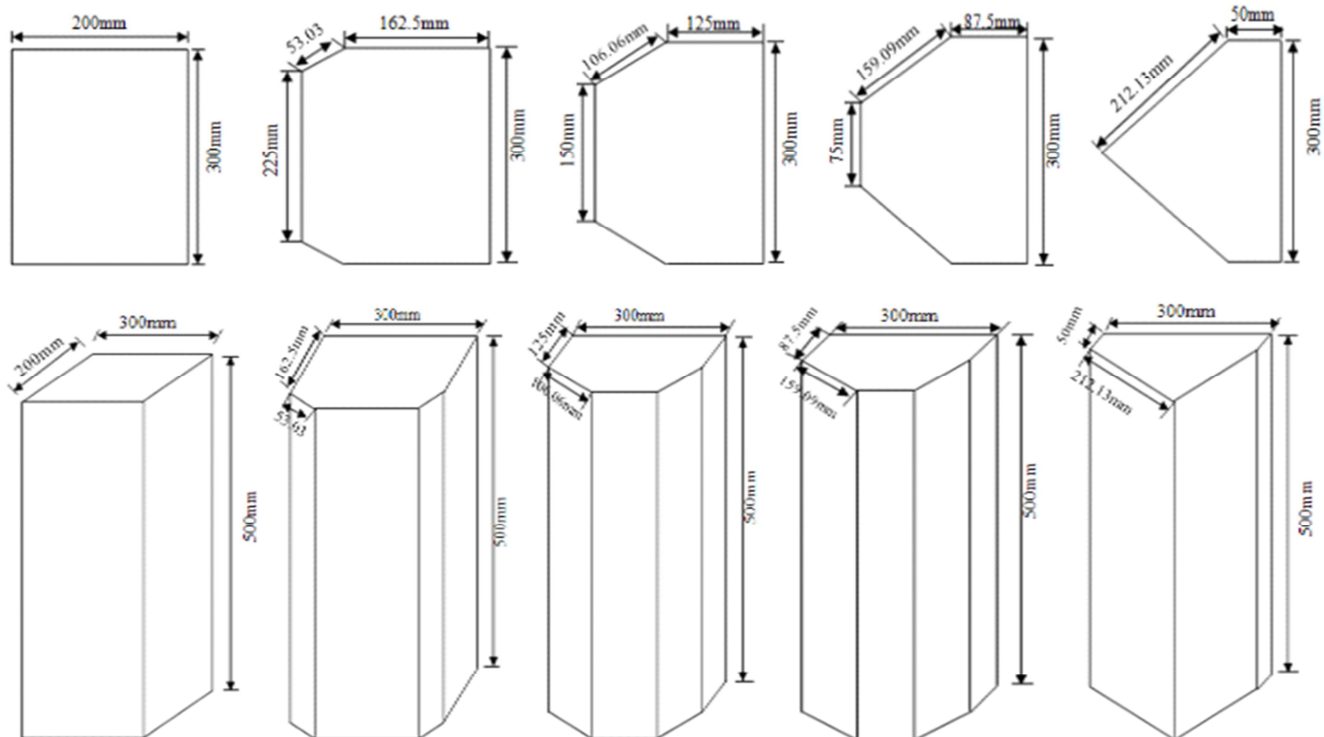


Figure 3. Plan and Isometric elevation dimensions of models.

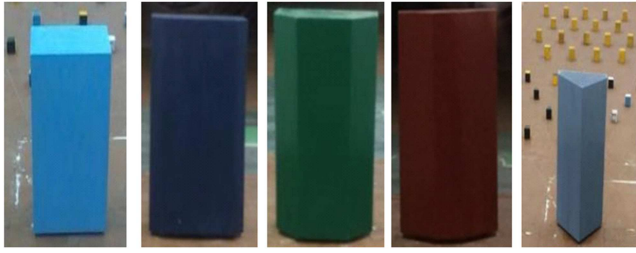


Figure 4. Actual Rigid plywood models for force measurements.

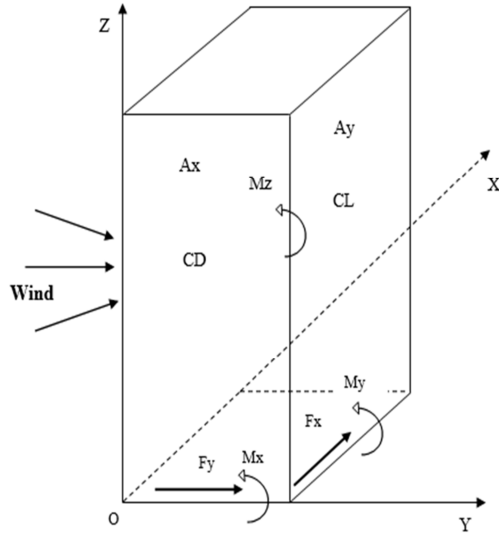


Figure 5. Projected Area, Static Response, and Force Coefficient Designation.

5.7. Evaluation of Drag-Force and Lift-Force Coefficients

Drag-force coefficients ( $C_D$ ): is a non-dimensional force-coefficient due to along-wind force, drag forces ( $F_x$ ) and estimated using the following expression,

$$C_D = \frac{F_x}{0.5 * \rho * V_{ref}^2 * A_x} \tag{1}$$

Lift-Force Coefficients ( $C_L$ ): is a non-dimensional force-coefficient due to across-wind, lift forces ( $F_y$ ) and estimated using the following expression,

$$C_L = \frac{F_y}{0.5 * \rho * V_{ref}^2 * A_y} \tag{2}$$

To achieve non-dimensionality of coefficients  $F_x$  and  $F_y$  are multiplied by,  $g=9.81m/sec$ . Projected area is the maximum projected surface area contributing resistance to wind load in particular wind incidences.

Where  $\rho=$  density of air ( $1.2kg/m^3$ ),

$V_{ref}$  = the mean wind velocity measured at boundary layer depth in the wind tunnel,

$A_x=$  the projected area of the model in an along-wind direction,

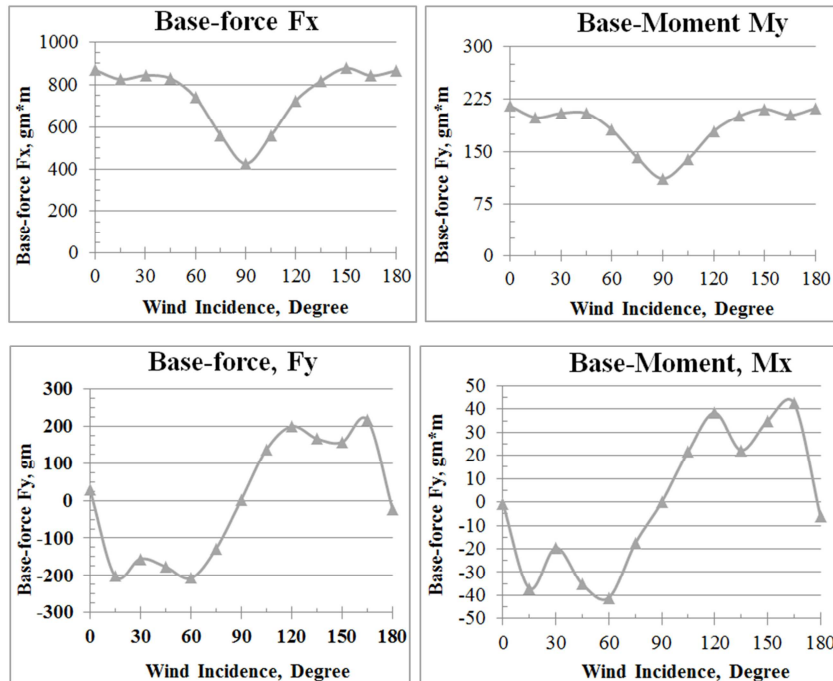
$A_y=$  the projected area of the model in an across-wind direction.

$F_x$  and  $F_y$  are forces in gram from the results of force measurements.

6. Results

6.1. Rectangular Model with Sharp Corner

The base force  $F_x$ , is maximum at  $0^\circ$  and  $180^\circ$  where, base force  $F_y$ , is maximum at  $15^\circ$  and  $165^\circ$ . The base force  $F_x$  is minimum at  $90^\circ$  and the base force  $F_y$  is minimum at  $90^\circ$ . The maximum and minimum value of base moments  $M_y$  and  $M_x$  is identical to the maximum and minimum value of  $F_x$  and  $F_y$  respectively. The maximum twisting moment occurs at  $75^\circ$ , whereas the minimum twisting moment occurs at  $0^\circ$ .



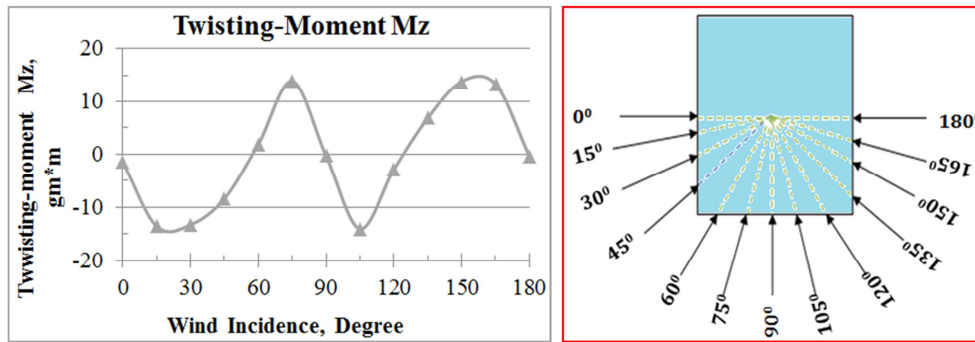


Figure 6. Variation of static response for sharp edge rectangular model.

**6.2. Rectangular Model with a Chamfered Edge, (37.5\*37.5) mm**

The base force  $F_x$ , is maximum at  $180^\circ$  due to the unchamfered edge of another longer side, whereas base force  $F_y$ , is maximum at  $120^\circ$ . The base force  $F_x$  is minimum at  $90^\circ$

and the base force  $F_y$  is minimum at  $180^\circ$ . The maximum and minimum value variations of base moments  $M_y$  and  $M_x$  is identical with the variation of corresponding base force values  $F_x$  and  $F_y$  respectively. The maximum twisting moment occurs at  $30^\circ$ , whereas the minimum  $M_z$  occurs at  $0^\circ$ .

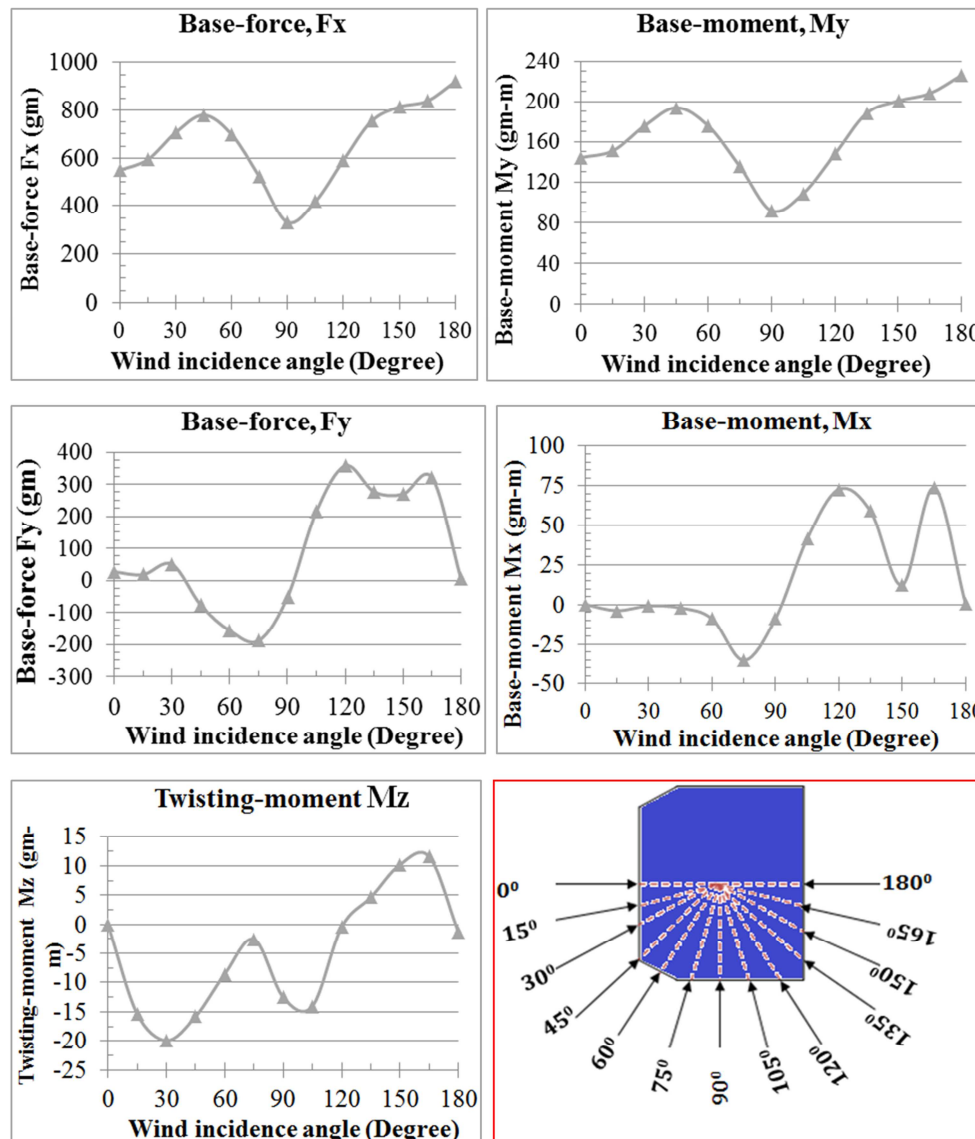


Figure 7. Variation of static response for 37.5mm\*37.5mm chamfered model.

**6.3. Rectangular Model with a Chamfered Edge, (75\*75) mm**

The base force Fx, is maximum at 180° due to the un-chamfered edge of another longer side, whereas base force Fy, is maximum at 135°. The base force Fx is minimum at 90° and the base force Fy is minimum at 0° and 180°. The

maximum and minimum value variations of base moments My and Mx is identical with the variation of corresponding base force values Fx and Fy respectively. The maximum twisting moment occurs at 90°, whereas the minimum twisting moment occurs at 180°.

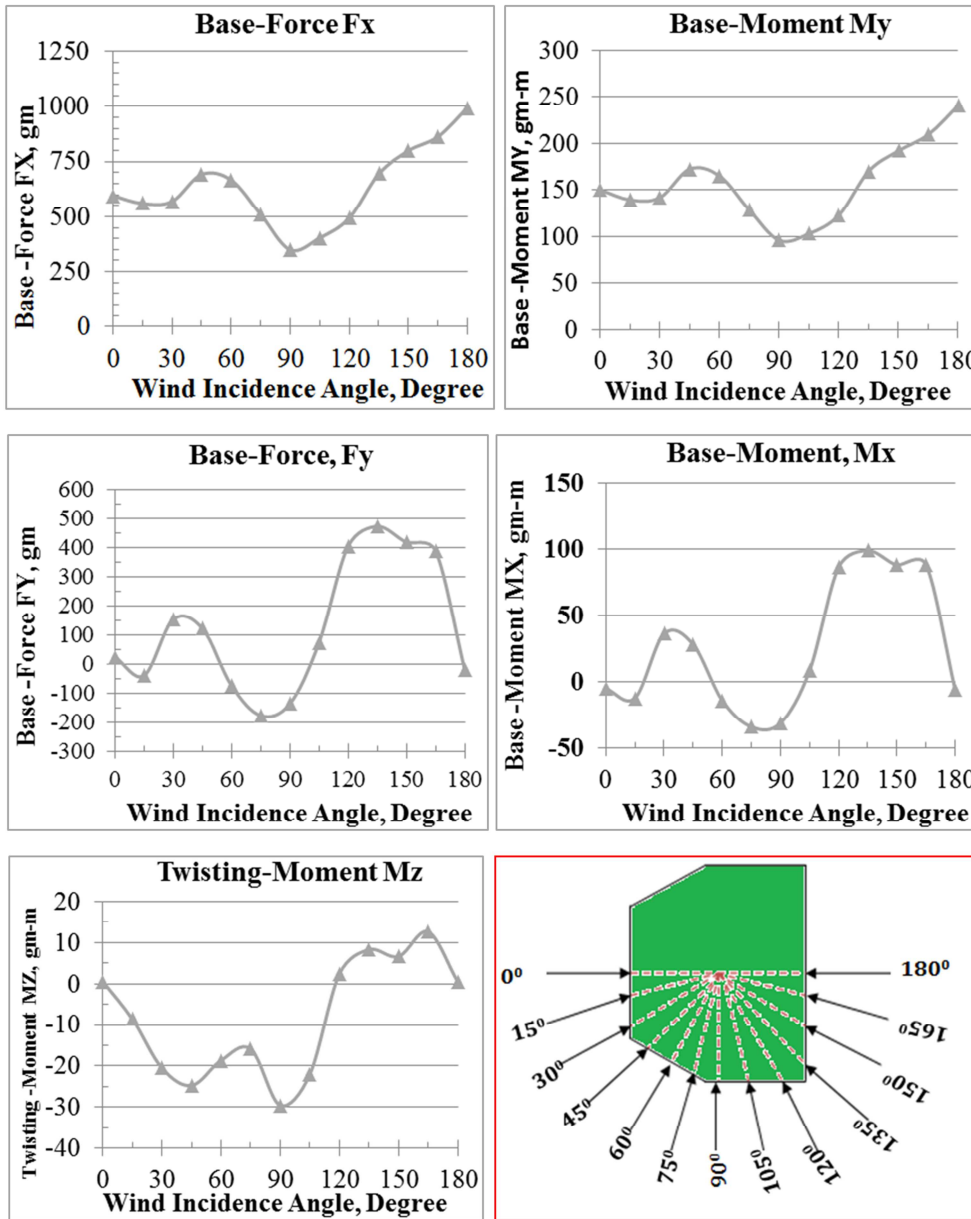


Figure 8. Variation of static response for 75mm\*75mm chamfered model.

**6.4. Rectangular Model with a Chamfered Edge, (112.5\*112.5) mm**

The base force Fx, is maximum at 180° due to the un-chamfered edge of another longer side, whereas base force Fy, is maximum at 135°. The base force Fx is minimum at 90°

and the base force Fy is minimum at 180°. The maximum and minimum value variations of base moments My and Mx is identical with the variation of corresponding base force values Fx and Fy respectively. The maximum twisting moment occurs at 90°, whereas, minimum twisting moment occurs at 15°.

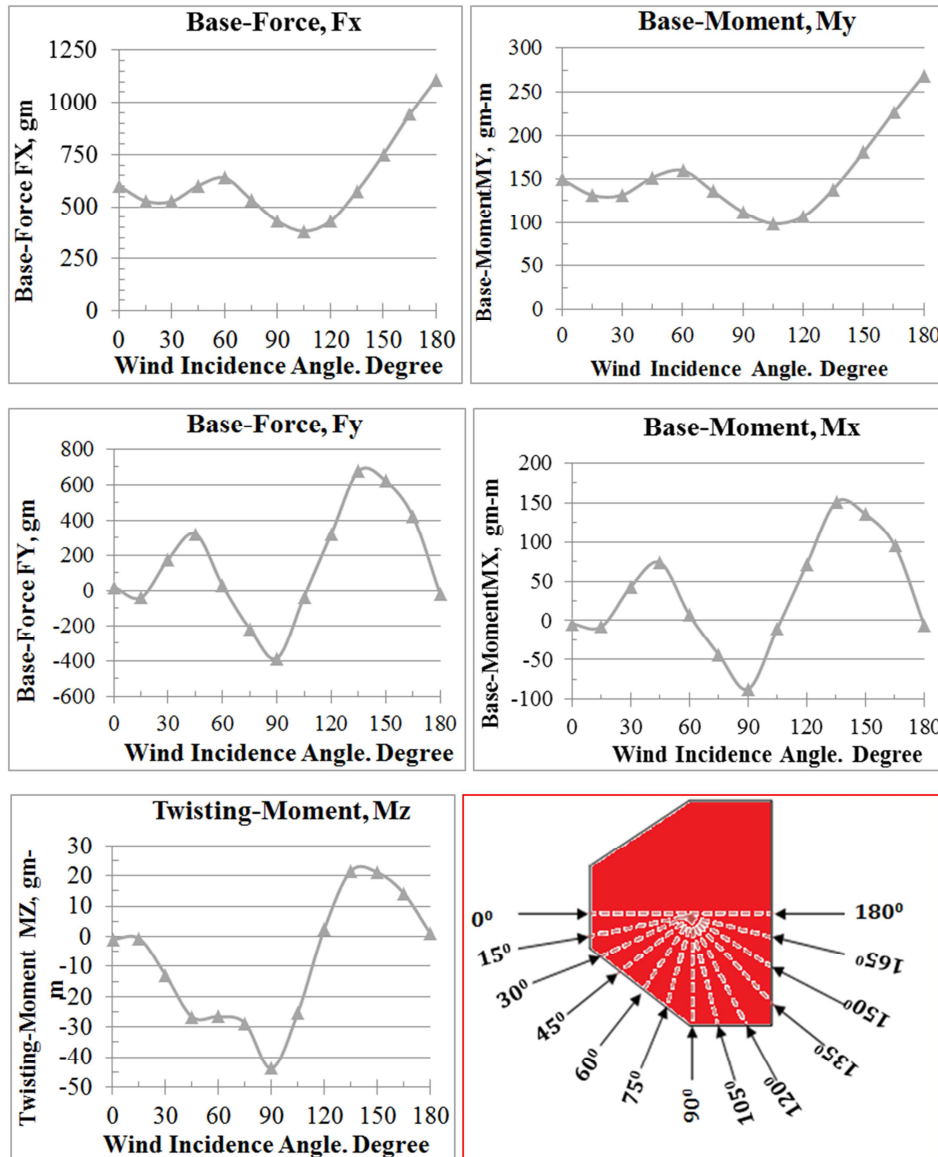
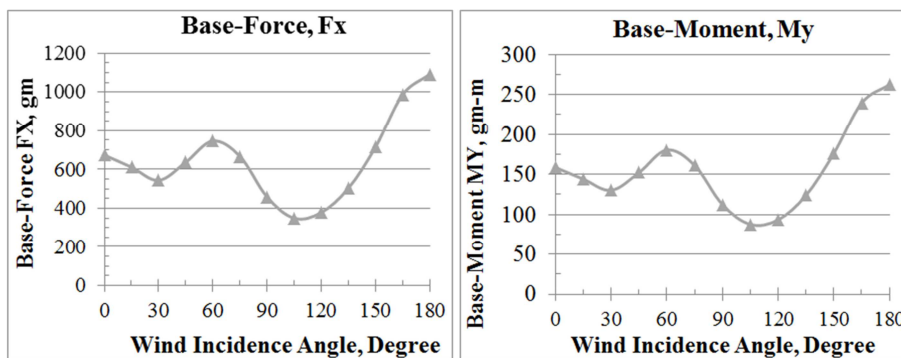


Figure 9. Variation of static response for 112.5mm\*112.5mm chamfered model.

**6.5. Rectangular Model with a Chamfered Edge, (150\*150) mm**

The base force Fx, is maximum at 180° due to the unchamfered edge of another longer side, whereas base force Fy, is maximum at 150°. The base force, Fx is minimum at

105° and the base force Fy is minimum at 180°. The maximum and minimum variations of base moments My and Mx is identical with the variation of corresponding base force values Fx and Fy respectively. The maximum twisting moment occurs at 90°, whereas the minimum twisting moment occurs at 180°.



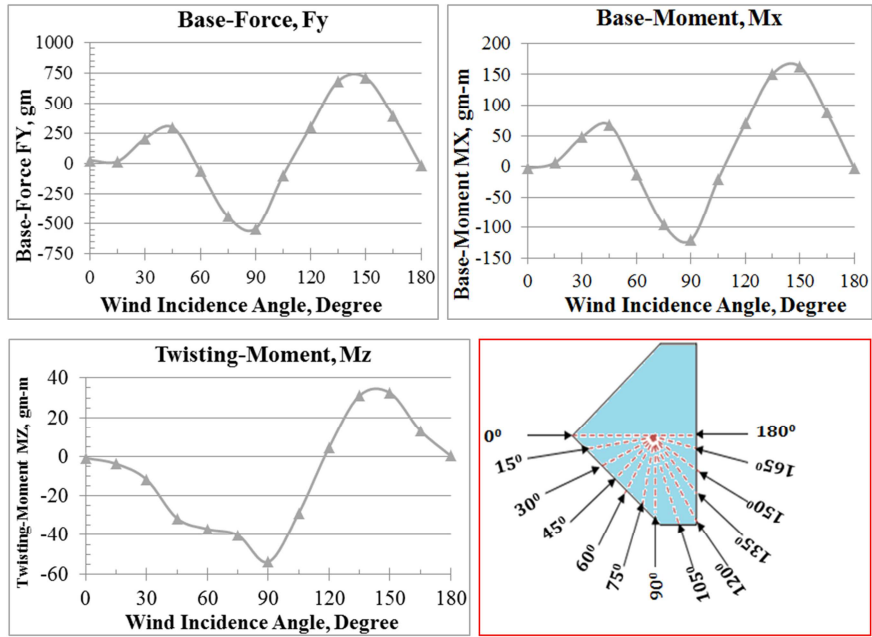


Figure 10. Variation of static response for 150mm\*150mm chamfered model.

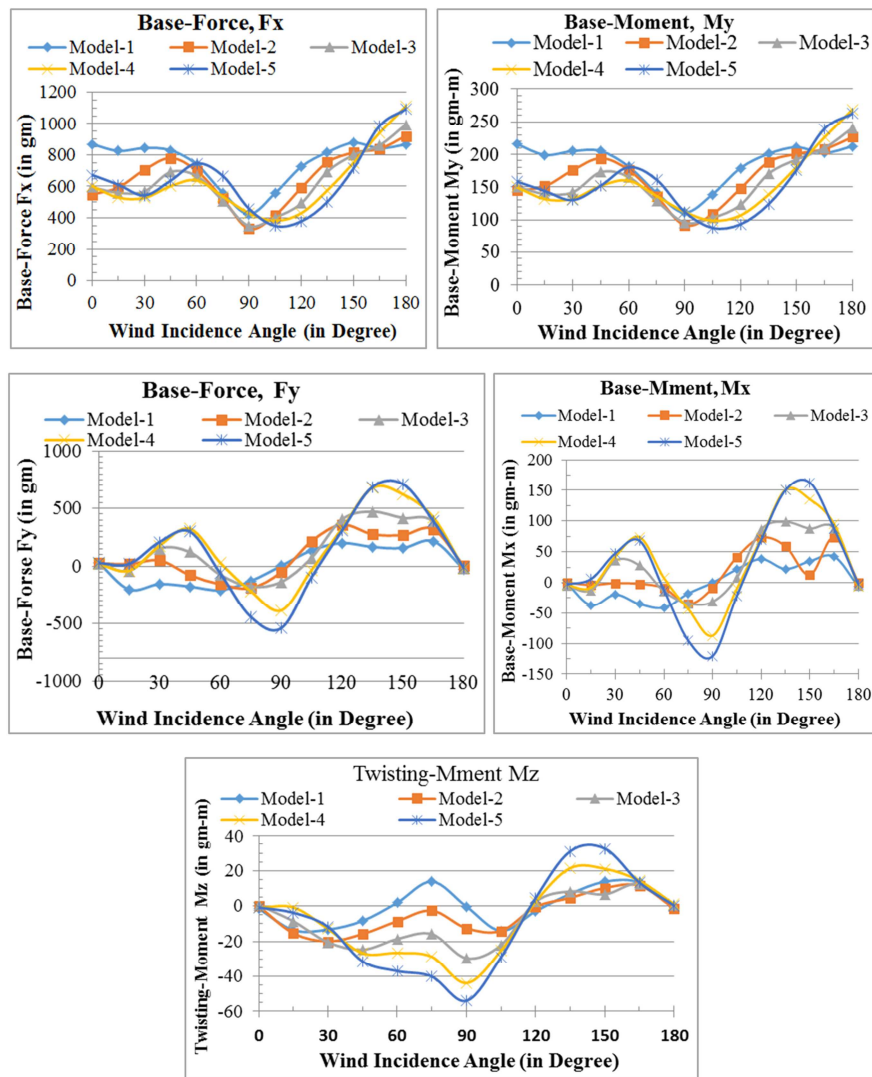


Figure 11. Variation of wind loads on all models.

Minimum Static Response						Maximum Static Response					
Models	Mz	Fx	MY	Fy	Mx	Models	Mz	Fx	MY	Fy	Mx
Model-1	0.29	424.61	111.00	2.13	42.47	Model-1	-14.02	877.70	215.79	216.67	42.47
Model-2	0.02	331.19	91.86	5.32	73.77	Model-2	19.95	920.70	226.24	357.61	73.77
Model-3	0.47	348.81	96.04	19.92	98.65	Model-3	29.57	993.78	240.53	471.18	98.65
Model-4	0.75	381.84	98.73	18.92	150.71	Model-4	43.80	1110.40	268.76	677.25	150.71
Model-5	0.31	349.44	87.76	14.02	162.83	Model-5	53.88	1092.27	262.62	712.40	162.83

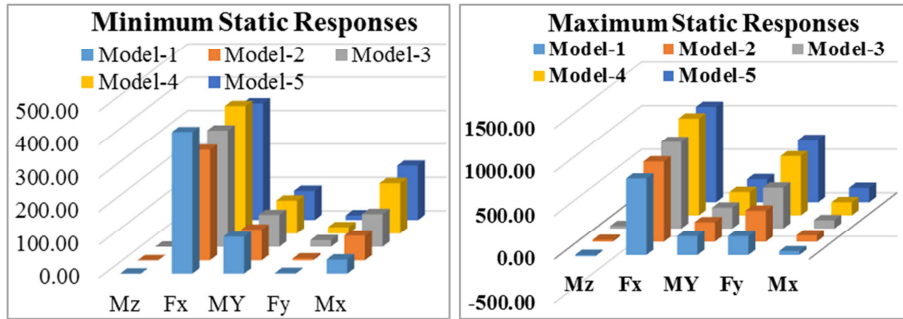


Figure 12. Variation of maximum base forces, base moments, and twisting moment.

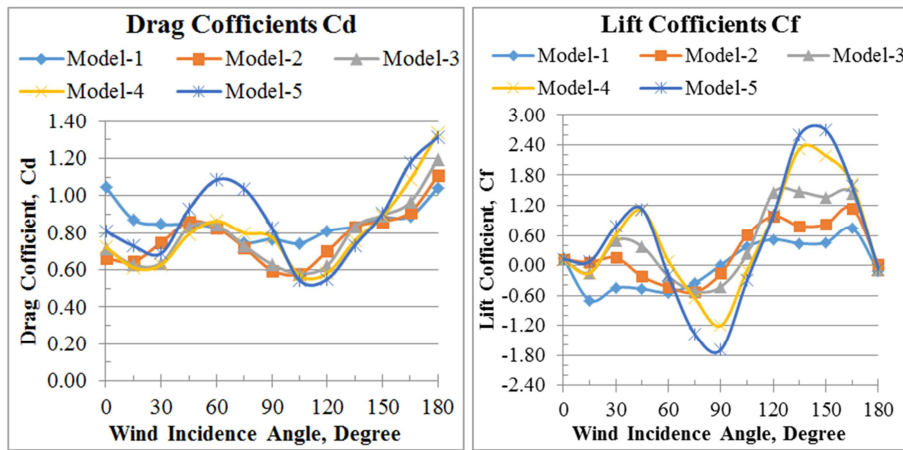


Figure 13. Drag force coefficients, CD and lift force coefficients, CL.

Model No.	C <sub>D</sub> max	C <sub>D</sub> min	C <sub>L</sub> max	C <sub>L</sub> min
Model-1	1.04	0.74	0.29	-0.27
Model-2	1.11	0.58	0.44	-0.21
Model-3	1.2	0.58	0.57	-0.2
Model-4	1.34	0.57	0.89	-0.46
Model-5	1.31	0.54	1.04	-0.65

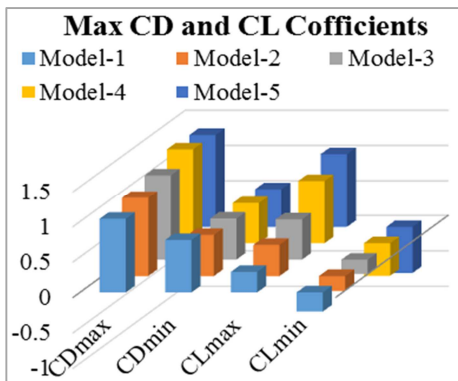


Figure 14. Maximum Drag force coefficients, CD and maximum lift force coefficients, CL.

## 7. Discussion

The maximum and minimum variations of base force, base moment, and twisting moment across each model are discussed below as a function of wind incidence angle and model edge configuration (chamfering size).

The base force  $F_x$ , a force in the direction of the wind is maximum at  $180^\circ$  and the minimum value is observed at  $90^\circ$  for models 1 to 3 and at  $180^\circ$  for models 4 and 5. The maximum base force  $F_x$  in model-5 is around 1.25 times that of model-1. The base force  $F_y$ , force across the direction of the wind is maximum at  $165^\circ$  at model-1,  $120^\circ$ ,  $135^\circ$  and  $150^\circ$  for model one up to model five respectively. The base force  $F_y$  is minimum at  $90^\circ$  for model-1 and at  $180^\circ$  for the rest models. The maximum base force  $F_y$  in model-5 is around 3.3 times that of model-1. The maximum and minimum value variation of  $M_x$  and  $M_y$  shows a similar pattern with the variation of maximum and minimum value of  $F_y$  and  $F_x$  respectively. The twisting moment  $M_z$  is maximum at  $75^\circ$  for model-1, at  $30^\circ$  for model-2, and at  $90^\circ$  for model-3 to 5. The twisting moment  $M_z$  is minimum at  $90^\circ$ ,  $0^\circ$ ,  $180^\circ$ ,  $15^\circ$  and  $180^\circ$  for each model respectively. The maximum

twisting moment  $M_z$  in model-5 is around 3.84 times that of model-1.

## 8. Conclusion

From this rigorous experimental study, the author concludes the following important findings.

- 1) As compared with a rectangular model with sharp corners maximum percentage of increase in base force  $F_x$  occurs in model-4, whereas the minimum base force  $F_x$  occurs in model-2.
- 2) The maximum twisting moment is observed in model-5 which is 3.84 times that of model-1 because, the mass and the stiffness of the structure is decreased due to chamfering. this indicates in designing more slender building, the effect of wind should be carefully considered.
- 3) The maximum drag-force coefficient is 1.34 in model 4 and the minimum is 0.54 in model 5 whereas the maximum Lift-force coefficient is 1.04 in model 5 and the minimum is -0.20 in model 3.
- 4) Maximum wind load is obtained in the face where the exposed projected frontal area is large.
- 5) Chamfering size has a great effect in modifying wind loads, even at the same incidence due to the shielding effect.
- 6) Position of models at critical wind incidences like  $0^\circ$ ,  $90^\circ$  and  $180^\circ$  gives maximum and minimum magnitude of wind loads. The direction of wind as well as the position of the building is an important factor in addition to the chamfered edge modification for the static responses of the building for wind load.
- 7) The maximum and minimum drag and lift force coefficients are aligned with maximum and minimum base force  $F_x$  and  $F_y$  respectively.
- 8) The lift-force coefficient for rectangular buildings with the same aspect ratio at  $0^\circ$  wind incidence from IS: 875, Part-3-2015 is 1.3, whereas the experimental force coefficient is 1.05.
- 9) The results from this research helps to decide the orientation of such building with respect to wind direction and the types of structural system to be used to resist external wind load.
- 10) The result from this experimental study is very helpful, for the design of rectangular tall building with vertical edge modification under wind load in which the wind design codes couldn't access.
- 11) The result from this paper supports wind load Code standards for high rise building design.

## Acknowledgements

I acknowledge the IIT ROORKEE wind engineering laboratory technicians for their help during the experimental setup and I also my staff at Debre Tabor University who helped me during the process of writing this paper.

## References

- [1] K. C. S Kwok 1998, Effect of building shape on wind induced responses of tall buildings, *Journal of Wind Engineering and Industrial Aerodynamics*, 28, 381-390.
- [2] Amin, JA and Ahuja, Ashok Kumar. (2010). aerodynamic modifications to the shape of the buildings: a review of the state-of-the-art, *Asian journal of civil engineering*.
- [3] Bhatnagar, N. K. (2011), "Effect of Geometrical Shapes on Wind Loads on Buildings" Indian Institute of Technology Roorkee, India, September 2011.
- [4] J. A. Amin • A. K. Ahuja (2014), Characteristics of wind forces and responses of rectangular tall buildings, *international journal of advanced structural Eng.*
- [5] Mooneghi, Maryam Asghari and Kargarmoakhar, Ramtin. (2016). Aerodynamic mitigation and shape optimization of buildings. *Journal of building engineering*, 6, 225-235.
- [6] Ashutosh, Sharma and Hemant, Mittal and Ajay, Gairola. (2018). Mitigation of wind load on tall buildings through aerodynamic modification: Review. *Journal of Building Engineering*, 18, 180-194.
- [7] Li, Yi and Li, Chao and Li, Qiu-Sheng and Song, Qian and Huang, Xuan and Li, Yong-Gui. (2020). Aerodynamic performance of CAARC standard tall building model by various corner chamfers}. *Journal of Wind Engineering and Industrial Aerodynamics*, 202, 104197.
- [8] Thordal, Marie Skytte and Bennetsen, Jens Chr and Capra, Stefano and Kragh, Andreas K and Koss, H Holger H. (2020). Towards a standard CFD setup for wind load assessment of high-rise buildings: Part 2--Blind test of chamfered and rounded corner high-rise buildings. *Journal of Wind Engineering and Industrial Aerodynamics*, 205, 104282.
- [9] Mohammad Jafaria, and Alice Alipoura, 2020, Methodologies to Mitigate Wind-induced Vibration of Tall Buildings: A State-of-the-art Review Mohammad, Elsevier.
- [10] Jamaluddeen and Rajiv Banerjee, 2021 An Analytical Study on Effect of Wind Load for Tall Building, *International Research Journal of Engineering and Technology*, Vol. 8.
- [11] Astha Verma, Rahul Kumar Meena, Hrishikesh Dubey, Ritu Raj, and S. Anbukumar, 2022, Wind Effects on Rectangular and Triaxial Symmetrical Tall Building Having Equal Area and Height, *hindawi*.
- [12] Meena, Rahul Kumar and Raj, Ritu and Anbukumar, S. (2022). Wind Excited Action around Tall Building Having Different Corner Configurations. *Advances in Civil Engineering*, 2022.
- [13] Al-masoodi, Aiman HH and Alkhatib, FH and Shafiq, N and Wahab, MMA. (2022). The Aerodynamic Performance of Tall Buildings by Utilizing Aerodynamic Modifications-A Review Study. *IOP Conference Series: Earth and Environmental Science*, 1022, 012046.
- [14] IS: 875-part-3 (2015) "Code of practice for design loads (other than EQ) for Building & Structure-Wind loads"
- [15] AS/NZS: 1170.2 (2002), "Structural Design Actions, Part 2 - Wind Actions".